

# Breast Ultrasound Elastography using Full Inversion Based Elastic Modulus Reconstruction

Seyed R. Mousavi, Hassan Rivaz, Ali Sadeghi-Naini, Gregory J. Czarnota, and Abbas Samani

**Abstract**—Several cancer types, including breast cancer, are associated with tissue structural changes that yield tissue stiffening. Clinical breast examination (CBE) is a physical examination of the breast to find palpable breast tumors. This test lacks accuracy necessary for effective assessment and diagnosis of breast cancer. To develop an effective breast cancer diagnostic technique, an imaging method is proposed that maps the distribution of breast tissue relative elasticity modulus. Unlike CBE, this technique is quantitative, hence it is expected that its accuracy is independent of the physician’s experience. The proposed technique is a quasi-static elastography technique which uses radiofrequency data acquired through ultrasound imaging to determine both axial and lateral tissue displacements resulting from tissue mechanical stimulation. These displacements serve as input data for elastography image reconstruction. The reconstruction technique is developed using a full inversion framework where elastic tissue deformation equations are inverted using an iterative process. Each iteration in this process involves stress computation using finite element analysis followed by updating elastic modulus until convergence is achieved. The proposed technique was validated by two tissue mimicking phantom studies before it was successfully applied to a clinical case. The two independent phantom studies demonstrated the robustness of the proposed method demonstrated by reconstruction errors of less than 12%. Elastic modulus images of the clinical case were compared to corresponding B-modes images where cancerous areas were identified as hypo-echoic areas. This comparison indicated

marked tissue stiffening in those areas. Results obtained from the phantom and patient studies conducted in this study indicate that the proposed method is reasonably accurate, hence the technique can be potentially used for quantitative assessment of breast cancer. The elasticity reconstruction algorithm developed in this work can be easily implemented on clinical ultrasound systems with no requirement to any additional hardware attachment for mechanical stimulation or data acquisition. As such, it can be applied as a low cost and potentially widely available technology for breast cancer diagnosis.

**Index Terms**—Breast, ultrasound elastography, data inversion, finite element.

## I. INTRODUCTION

**B**REAST cancer is the most common type of non-dermal cancer and the major cause of cancer-related death among women globally [1]. North America has one of the highest incidence breast cancer rates in the world, making breast cancer awareness a high priority. Only in the USA, 527 women are expected to be diagnosed with breast cancer while 110 women will die of it per day [1]. Central to the importance of breast cancer diagnosis is the fact that almost one-third of the latter group could survive if their cancer is detected and treated early. In a worldwide context, this translates into nearly 400,000 lives who could be saved every year as a result of early detection [1]. As such, developing techniques that can help to detect and diagnose breast cancer at early stages can have a great impact on survival and quality of life of breast cancer patients.

Conventional breast cancer screening and detection techniques such as clinical breast examination (CBE) and X-ray mammography are known to have low sensitivity [2]. Breast magnetic resonance imaging (MRI) is a more sensitive modality for breast cancer detection. There is an increasing interest in using breast MRI for breast cancer screening for women with high risk of breast cancer, however, MRI is costly and has been shown to have low specificity for breast cancer diagnosis [2]. Dynamic contrast-enhanced MRI (DCE-MRI) has been demonstrated to provide a good sensitivity and specificity for differentiation of benign versus malignant lesions, due to altered angiogenesis mechanisms in tumours [3]. However, in addition to being costly, DCE-MRI requires injection of exogenous contrast agents to provide such contrast.

Manuscript submitted April 10, 2017. This work was supported in part by the Natural Sciences and Engineering Research Council of Canada (NSERC).

A. Samani is with the Department of Electrical and Computer Engineering, Department of Medical Biophysics, and Graduate Program in Biomedical Engineering, Western University, London, Ontario, Canada, N6A 5B9, and with the Imaging Research Laboratories, Robarts Research Institute (RRI), London, Ontario, Canada, N6A 5K8 (e-mail: asamani@uwo.ca).

G. J. Czarnota and A. Sadeghi-Naini are with the Departments of Medical Biophysics and Radiation Oncology, University of Toronto, Toronto, Ontario, Canada, M4N 3M5, and with Sunnybrook Research Institute and Odette Cancer Centre, Sunnybrook Health Sciences Centre, Toronto, Ontario, Canada, M4N 3M5 (e-mails: gregory.czarnota@sunnybrook.ca and ali.sadeghi@sri.utoronto.ca).

H. Rivaz is with the Department of Electrical and Computer Engineering, Concordia University, Montreal, Quebec, Canada, H4B 1R6, and with PERFORM Centre, Concordia University, Montreal, Quebec, Canada, H4B 1R6 (e-mail: hrivaz@ece.concordia.ca).

S. R. Mousavi is with the Department of Medical Biophysics, Western University, London, Ontario, Canada, N6A 5C1 and with the Department of Medical Biophysics and Radiation Oncology, University of Toronto, Toronto, Ontario, Canada, M4N 3M5, and with Sunnybrook Research Institute and Odette Cancer Centre, Sunnybrook Health Sciences Centre, Toronto, Ontario, Canada, M4N 3M5.

An alternate imaging technique for breast cancer detection employs tissue stiffness as contrast mechanism. The technique is founded on the fact that alterations in breast tissue stiffness are frequently associated with pathology [4], [5]. This was demonstrated by stiffness measurement studies of *ex vivo* breast tissue samples conducted by Krouskop et al. [6] and Samani et al. [7], [8]. Based on their measurements, there is a significant difference between the Young's moduli of breast tumor and healthy breast tissues. As such, imaging breast tissue stiffness or breast elastography can be potentially used as a non-invasive breast cancer diagnosis method with a high efficacy. After development of elastography techniques [9], breast elastography was introduced as one of the first reported clinical applications developed based on the elastography concept. Two alternative methods of quasi-static and harmonic elastography were proposed. In the quasi-static methods, the tissue is mechanically stimulated very slowly and the resulting tissue deformation data are acquired using imaging modalities such as MR or ultrasound (US). In harmonic elastography, a mechanical wave is induced in the tissue and either vibration amplitude or wave speed is measured using MRI or US imaging techniques. In both cases, acquired data is used to estimate the tissue mechanical properties (e.g. Young's modulus).

Several feasibility studies [10]-[14] aiming at breast cancer diagnosis which involved harmonic US elastography were reported. Among relevant groups, Sinkus et al. [15], [16] and Van Houten et al. [17] proposed harmonic MR elastography techniques to measure the viscoelastic shear properties of *in vivo* breast lesions. While harmonic elastography techniques provide information related to tissue viscosity properties that may potentially carry more diagnostic information to characterize a breast lesion, they usually require additional hardware attachments for wave generation in addition to ad hoc software including specialized pulse sequences for MR elastography. These techniques also involve approximations which lead to elastic modulus reconstruction formulation based on the wave form and propagation characteristics. Other groups developed quasi-static elastography methods in the form of mechanical imaging [18], strain imaging [19]-[25] and full inversion techniques [26], [27] for breast cancer diagnosis. In mechanical imaging [18], mechanical parameters of the breast lesions were estimated using contact stress patterns on breast surface measured through a force sensor array pressed against the breast. This imaging approach is based on the premise that temporal and spatial changes in the stress pattern allow detection of internal structures with different elastic properties and assessing their geometrical characteristics. Strain imaging is based on a simplifying assumption of uniform tissue stress distribution under which tissue stiffness is proportional to its strain reciprocal. Since stress spatial variation developed within the breast tissue during mechanical stimulation is far from uniform, strain imaging does not provide reliable quantitative tissue stiffness information necessary for high sensitivity and specificity in breast cancer diagnosis. Full-inversion based elastography techniques on the other hand, account for tissue stress variation, permitting

reconstruction of quantitative maps of elasticity modulus. One difficulty with inversion based quasi-static elastography methods is that they are computationally intensive, unstable and hard to implement. To reduce the complexity of the elastography inversion algorithms, Samani et al. [28] developed a MR-based iterative inversion algorithm for breast elastography. This technique was later implemented based on an ultrasound platform [29] as a step to develop near real-time, low cost and widely available imaging system. The algorithm was shown to be robust, however, it requires image segmentation for healthy and tumor tissue delineation. This requirement is not easy to fulfill, especially with US imaging. To address these issues, our group [30] proposed an unconstrained full inversion algorithm for ultrasound elastography. The method was validated by tissue mimicking phantom studies before it was applied to clinical prostate data.

In this paper, we adapt our recently-proposed methodology for unconstrained full inversion-based breast elastography. Unlike with the prostate, ultrasound is capable of imaging only a portion of the breast due to its limited field of view (FOV). As such, only a portion of the breast geometry is accessible which precludes the possibility of identifying boundaries where force and displacement boundary conditions are necessary for modulus reconstruction. To deal with this issue, Samani et al. [31] approximated the breast geometry with various trapezoidal regions while assumed that the stress is negligible outside those regions. To assess the accuracy of this geometric approximation, they investigated its impact on the reconstruction accuracy by conducting a simulation study. The simulation study involved comparing the results obtained using approximated breast geometries with the results from actual geometry. They concluded that the best results will be achieved if the breast geometry is approximated with a trapezoid of 35° side angle and the same depth as the FOV. Also for good results, the sonographer should move the probe around the breast surface until she/he captures an image where the tumour is positioned approximately in the center of the FOV. Mei et al. [32] developed a full inversion based elastography technique which requires displacement data measured on the boundary of the domain only. They evaluated their method using numerical phantom case studies.

In this work, we followed a different approach whereby the FOV axial and lateral displacements measured using ultrasound are used as prescribed boundary conditions in the modulus reconstruction. The proposed method was validated with two tissue mimicking phantom studies, one with a simple geometry and one with a more complex geometry mimicking the breast shape. The methods was also applied to clinical breast data and results were compared to the B-modes images where cancerous areas were identified as hypo-echoic areas. This preliminary clinical study demonstrated a good potential for clinical utility of the proposed method.

## II. METHODS

Samani et al. [28] presented a full inversion breast elastography technique where the breast Young's modulus

(YM) is reconstructed for cancer assessment. The proposed method was developed assuming that the tissue is linear elastic and isotropic undergoing small deformation. As such, the following equation, which is derived from Hooke's law, governs each point in the tissue domain:

$$\frac{1}{E} = \frac{\varepsilon_{11}}{\sigma_{11} - \nu\sigma_{22} - \nu\sigma_{33}} \quad (1)$$

In this equation  $\varepsilon$  and  $\sigma$  denote the tissue strain and stress developed under mechanical stimulation, respectively. Also, 1, 2 and 3 represent three orthogonal directions, and  $\nu$  is the tissue's Poisson's ratio. The tissue was assumed to be a near-incompressible material, hence  $\nu = 0.49$  was employed in the reconstruction. The reconstruction technique is iterative as the YM followed a  $E^{i+1} = f(E^i)$  recursive formulation used in each iteration, where  $f$  involves stress calculation using finite element method. Their approach followed a constrained reconstruction strategy by assuming that the YM is constant throughout the volume of each of the normal and pathological tissues, hence it required image segmentation to find each tissue volume. Although the assumption of tissue elasticity uniformity is reasonably good, accurate image segmentation necessary for accurate YM reconstruction is feasible with only high quality imaging modalities (e.g. MRI) and is not feasible with US imaging. To address this shortcoming, the same group proposed an unconstrained modulus reconstruction algorithm that does not require image segmentation. Their strategy of 2D YM reconstruction involves dividing the finite element model into subsets of  $n \times n$  finite element windows. The Young's modulus within each window is calculated iteratively as follows:

1- Starting with an initial YM value distribution, the stress field is computed using FE analysis.

2- With the axial strain field known from US imaging, the Young's modulus reciprocal value of each element is computed using:

$$\frac{1}{E} = \frac{\varepsilon_{11}}{\sigma_{11} - \nu\sigma_{22}} \quad (2)$$

3- The average Young's modulus reciprocal value of each  $n \times n$  element window is assigned to all elements in the window.

4- A Gaussian smoothing filter is applied to the FE domain to achieve a smooth distribution of the YM reciprocal values.

5- For each element the YM reciprocal is inverted to obtain the updated Young's modulus of the element.

6- Return to step 2 where the stress field is recomputed using the updated YM distribution.

This iterative process is repeated until the difference between two consecutive relative YM ( $E_{\text{tumor}}/E_{\text{background}}$ ) is less than a preset small value. The small value considered to ensure convergence in this work was set to 0.01 which was determined to achieve a compromise between reaching a plateau and clarity of tissue regions. The flow diagram of the proposed method is shown in Fig. 1.

#### A. Finite Element Modeling

The proposed method requires calculating the stress field in

the breast tissue while undergoing mechanical stimulation induced by the US probe. FE modeling was used for this purpose. FE modeling requires the geometry, tissue biomechanical properties and boundary conditions. In Samani et al. methodology [28], the whole breast geometry was acquired using MRI which facilitated finding the boundary conditions. With US imaging, however, only a portion of the breast can be imaged due to its limited FOV, precluding the possibility of finding free and fixed boundary conditions. To address this issue here, following a similar approach as applied in Oberai et al. [33], the reconstruction algorithm was modified by considering the acquired displacement data as prescribed boundary conditions along the boundaries of corresponding US images. These displacement boundary conditions included axial and lateral tissue displacements obtained using an US-based motion tracking technique.

The FE model was constructed based on 2D breast B-mode images. An example of such image is shown in Fig. 2(a). For FE analysis, a finite size rectangular model was considered mimicking the breast B-mode image. As the boundaries of the tumor tissue are unknown, the whole block was uniformly meshed as shown in Fig. 2(b). The size of finite elements was chosen to achieve a compromise between the accuracy and computational time. It was set to twice the distance between two consecutive ultrasound beams. Plane strain assumption was used in the finite element model of the reconstruction algorithm. Rivaz et al. [34] proposed an US-based motion tracking algorithm for calculating both axial and lateral displacements with reasonably high accuracy. All points on the four edges of the FOV were assigned prescribed displacement boundary conditions consistent with the axial and lateral displacements estimated using this US-based motion tracking method.

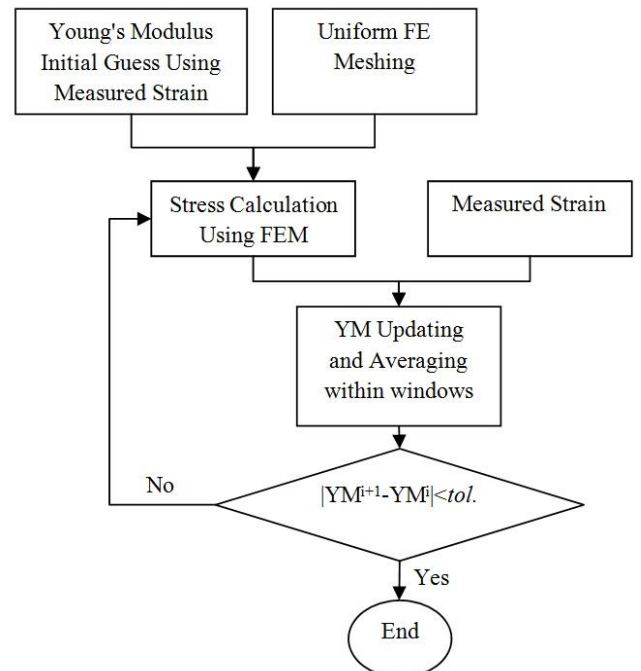


Fig. 1. Flowchart illustrating the unconstrained YM reconstruction procedure.

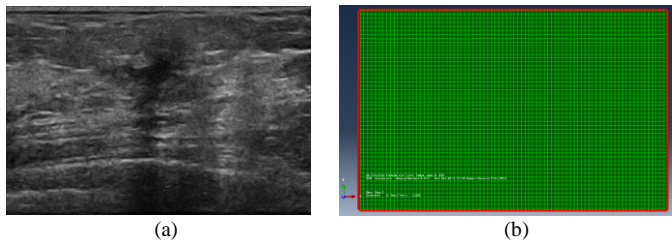


Fig. 2. Example of breast B-mode image (a) and corresponding finite element model with prescribed boundary conditions assigned to the FOV outline (b).

### B. Estimation of Axial and Lateral Displacements and Axial Strain Field

Ultrasound B-mode images, radiofrequency (RF) data, and clinical strain images were acquired using a Sonix RP ultrasound imaging system (Ultrasonix Medical Corporation, Richmond, BC, Canada). The axial strain fields used as “measured strain” in the flow chart and axial and lateral displacements used as boundary conditions to drive stress calculation were estimated using the method developed by Rivaz et al. [34]. In this method, the displacement values are calculated using two frames of ultrasound RF data corresponding to the pre- and post-compression states of tissue. The displacement values are calculated by minimizing a cost function that includes both amplitude similarity (data term) and displacement continuity (regularization/prior information). The minimization is performed through the following two steps [35]:

- 1- Dynamic programming (DP) is used to estimate integer displacement maps in both axial and lateral directions [35].
- 2- Continuous optimization is performed to obtain refined sub-sample displacement maps in both axial and lateral directions [34].

The axial strain map is then estimated by applying least-square minimization and Kalman filtering on the calculated displacement maps. Two attributes of this algorithm lead to high-quality displacement and strain maps and alleviates the effect of signal decorrelation. First, the prior information of displacement continuity helps guide the solution in regions with noisy data term. Second, the optimization is performed for an entire RF line wherein the displacement map of all

samples is calculated simultaneously whereas in classical correlation-based methods, displacement of each window is calculated independently which may fail in decorrelated windows.

### C. Tissue mimicking Phantom Study

The proposed elastography method was validated with two tissue mimicking phantom studies. In these studies the phantoms consisted of two parts which mimic the breast and tumor tissues. The phantom used in the first study had a simple block-shape geometry while the one used in the second study had a more complex breast-like geometry. These two phantoms are illustrated in Fig. 3.

The first phantom was manufactured by the Computerized Imaging Reference Systems (CIRS; Pacific Northwest X-ray Inc., Gresham, USA). A mechanical device along with the US probe was used for compressing the phantom with 0.1 inches steps. The second phantom was constructed in our lab using gelatin and agar dissolved in water. Table I shows the amount of each material used to construct the inclusion and background parts. A few drops of formaldehyde were added to the dissolved gelatin and agar to increase the melting point of the mixture and increase the phantom’s resistance against developing mould. Also, glycerol was added to the mixture to regulate the ultrasound wave speed in both the normal and tumor areas such that the wave speed is approximately 1540 m/s [36]. All the materials used to construct the phantom were manufactured by Sigma-Aldrich Co. LLC. To have better image contrast between normal and tumor areas, different concentrations of Sigmacel were added to the batch prepared for each tissue type to create nonuniform backscattering. For validation, a cylindrical sample was constructed from each batch. These samples were set to solidify under the same conditions for each tissue mimicking gelatin-agar material. These samples, underwent indentation tests to measure their YM values independently. Indentation was conducted using an apparatus consisting of a load cell along with a linear servo actuator and a computer controller. The actuator was equipped with a circular plane-ended indenter. The indenter, indented the cylindrical samples in steps with sinusoidal cycles of 0.1 Hz frequency while the indentation amplitudes and

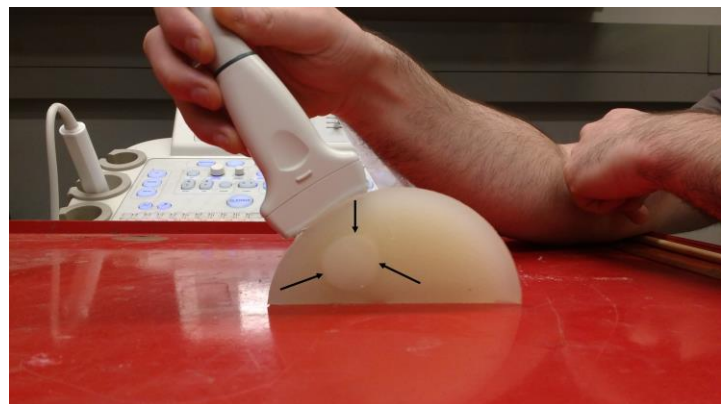
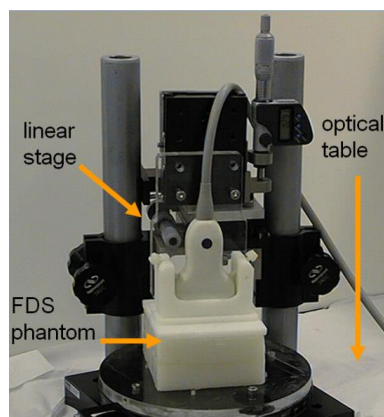


Fig. 3. Block-shape (left) and cylindrical (right) tissue mimicking phantoms consisting of an inclusion (indicated with 3 arrows) mimicking the tumor.

corresponding forces were saved for offline processing which involved inverse finite element modeling to calculate the YM of each sample. Unlike the first phantom, the second phantom was mechanically stimulated manually.

TABLE I

AMOUNTS OF DIFFERENT MATERIALS USED FOR CONSTRUCTING DIFFERENT REGIONS OF THE SECOND (CYLINDRICAL) PHANTOM

	Gelatin (g)	Agar (g)	Water (cc)	Glycerol (cc)	Sigmacel (g)	Formaldehyde (drop)
Background Tissue	24	5	400	20	2	1
Inclusion	12	4	200	10	2	1

#### D. Clinical Study

The proposed method was further evaluated using clinical data acquired from a breast cancer patient. The data were acquired in accordance with research ethics approval from Sunnybrook Health Sciences Centre, Toronto, ON, Canada. The patient underwent routine clinical imaging and biopsy to confirm a cancer diagnosis. Magnetic resonance imaging (MRI) of the breast was conducted as part of clinical care to measure the tumor size, using a 1.0 Tesla scanner (GE Healthcare, Waukesha, WI). The patient was confirmed with two tumors with measured sizes of  $2.3 \times 2.5 \times 2.5$  cm and  $1 \times 1 \times 0.7$  cm (AP  $\times$  CC  $\times$  TV) based on MRI. Ultrasound imaging was performed by a trained sonographer following standardized protocols for data acquisition. Ultrasound B-mode images and radio-frequency (RF) data were acquired from the affected breast using a Sonix RP system at a rate of 12 frames per second, utilizing a 6-cm-wide L14-5 transducer with a nominal centre frequency of 10 MHz. The RF data were collected prior to and after a quasi-static stimulation by probe for elastography. Ultrasound scan planes were acquired over the entire breast in 1-cm increments under the guidance of a physician.

### III. RESULTS

#### A. Tissue mimicking Phantom Study

The YM values of the inclusion and the background tissue for the first phantom were 56 kPa and 33 kPa ( $E_{inc}/E_{bkg} = 1.70$ ), respectively. The proposed unconstrained elastography method was applied to reconstruct this ratio. Fig. 4 illustrates acquired B-mode ultrasound image, axial and lateral displacement images, strain image and reconstructed elasticity image of this phantom. Based on the strain image, the tissue

YM ratio was obtained at 1.82, indicating an error of 7% for the tumor's relative elasticity. The YM ratio obtained from the reconstructed elasticity image is 1.86, indicating an error of 9%. It is noteworthy that the stress uniformity assumption for this simple phantom's geometry is a reasonably good approximation, which justifies the observed comparable errors.

Based on the indentation tests conducted to measure the YM of each tissue mimicking part in the second study with the cylindrical phantom, the YM values of the inclusion and the background were 25 kPa and 40 kPa ( $E_{inc}/E_{bkg} = 1.60$ ), respectively. Fig. 5 illustrates acquired B-mode ultrasound image, axial and lateral displacement images, strain image and the reconstructed YM image of this phantom. The tissue YM ratio was obtained at 1.83 based on the strain image, indicating an error of 14% for the tumor's relative elasticity. The YM ratio obtained from the reconstructed YM image was 1.49, indicating an error of only 7% for the tumor tissue. In this case, the accuracy achieved by the proposed method is significantly higher than that of the strain imaging.

#### B. Clinical Study

Fig. 6 shows a B-mode image acquired from the breast cancer patient, and the corresponding axial and lateral displacement images, strain image and the reconstructed YM image obtained. The hypo-intensity region in the B-mode indicates the tumor. The reciprocal strain ratio of this region relative to the background tissue was 1.4. The YM ratio of the tumor relative to the background tissue was calculated at 2.1 using the proposed reconstruction technique.

Fig. 7 illustrates a B-mode image, and the corresponding axial and lateral displacement images, strain image and reconstructed YM image acquired for the second tumour region of the patient. This scan showed a bigger hypo-intensity region indicating the tumor. The strain ratio of this region with respect to the surrounding background tissue was 2.7 whereas the corresponding YM ratio was calculated at 1.8 which is more reasonable.

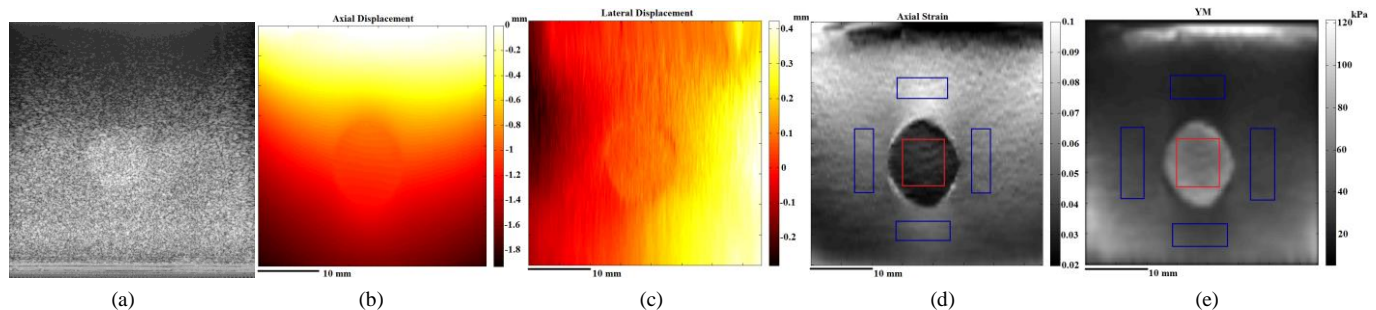


Fig. 4. B-mode Image (a), axial displacement image (b), lateral displacement image (c), axial strain image (d) and YM image (e) constructed using the proposed method. The ratio of the average strain value of the background (blue boxes) to the average strain value of the inclusion (red box) is 1.82. The ratio of the average YM value of the inclusion (red box) to the average YM value of the background (blue boxes) is 1.86. The true YM ratio is  $56/33 = 1.70$ .

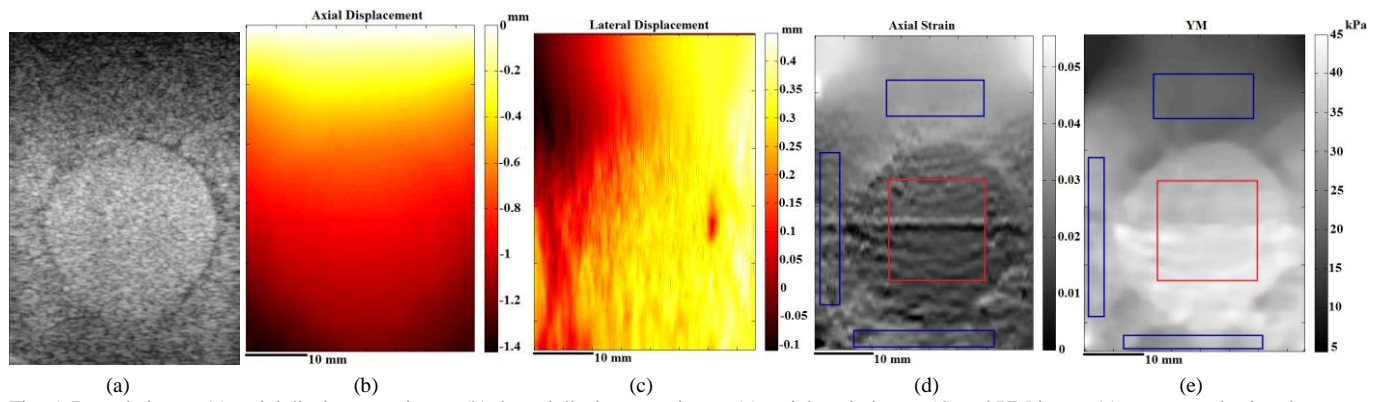


Fig. 5. B-mode image (a), axial displacement image (b), lateral displacement image (c), axial strain image (d) and YM image (e) constructed using the proposed method. The ratio of average strain value of the background (blue boxes) to average strain value of the inclusion (red box) is 1.83. The ratio of the average YM value of the inclusion (red box) to the average YM value of the background (blue boxes) is 1.49 while the true YM ratio is  $40/25 = 1.60$ .

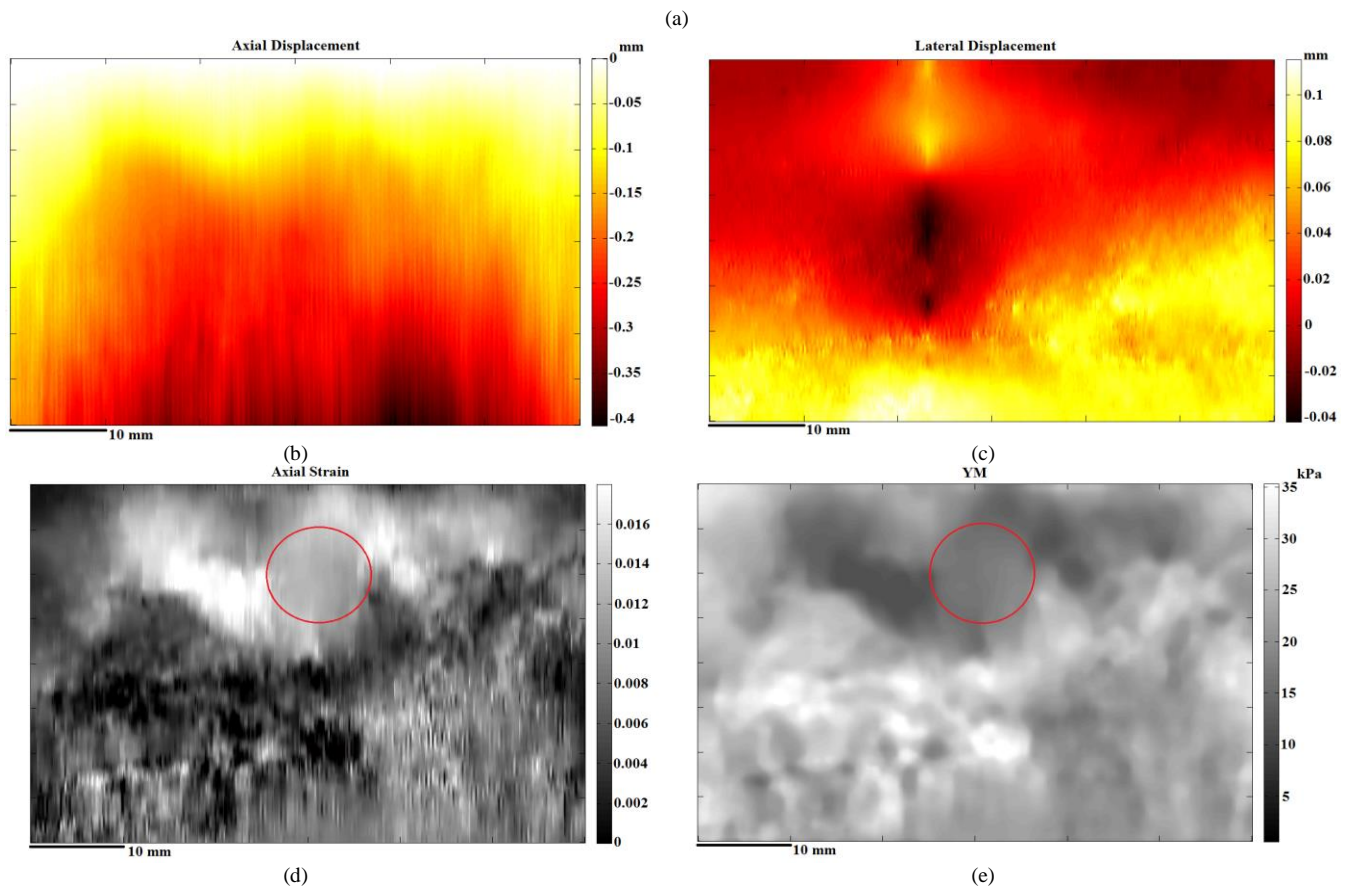
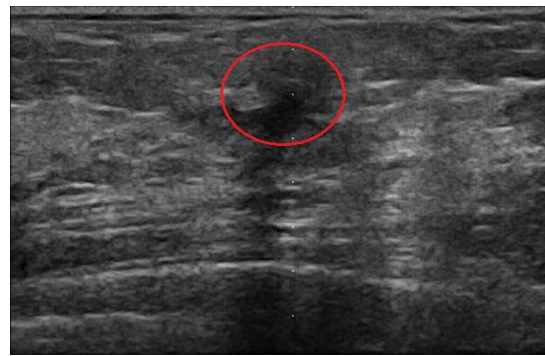


Fig. 6. B-mode image acquired from a breast cancer patient (a) and the corresponding images of axial displacement (b), lateral displacement (c), axial strain (d) and YM reconstructed using the proposed technique (e). The red circle encircles a tumor which appears harder than the surrounding tissue in the reconstructed YM image (YM ratio = 2.1).

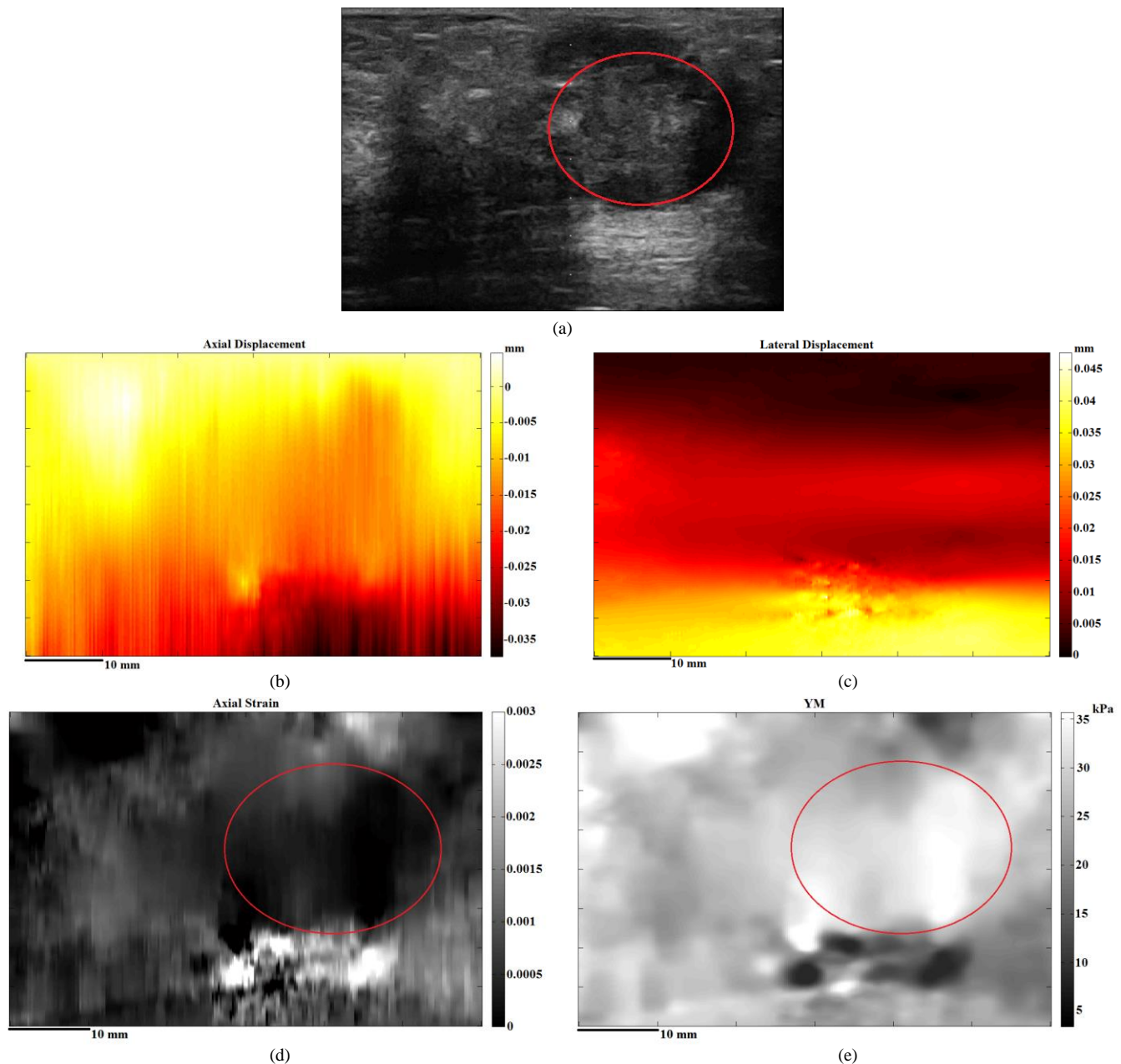


Fig. 7. B-mode image acquired from a second tumour region of the breast cancer patient (a) and the corresponding images of axial displacement (b), lateral displacement (c), axial strain (d) and YM reconstructed using the proposed method. The red circle encircles a tumor which appears harder than the surrounding tissue in the reconstructed YM image (YM ratio = 1.8).

#### IV. DISCUSSION AND CONCLUSIONS

A full inversion quasi-static technique was introduced in this paper for breast US elastography. The technique takes into account realistic boundary conditions and stress non-uniformity, leading to a reliable YM reconstruction. It only requires US RF signals at pre- and post-compression states that can be acquired using a clinical ultrasound system, with no additional hardware attachment. As such, it has the potential to be implemented as an add-on into standard ultrasound systems for effective breast cancer assessment. The advantage of the method compared to constrained elastography techniques [28], [29] is that it does not require

image segmentation for YM image reconstruction. This is critical for US elastography since exact tumor boundaries are frequently not clear in B-mode images. Eliminating the segmentation step also reduces computational complexity of the reconstruction. Compared to strain imaging, the method is more accurate especially with realistic clinical cases where tissue stress uniformity is a very poor assumption. However, the reconstruction algorithm is computationally more complex than strain imaging as it involves stress analysis using FE modeling. As such, in contrast to strain imaging, the method is not suitable for real-time applications unless parallel computing using GPU programming [37] is used.

Based on the tissue mimicking phantom studies, the

proposed US elastography method can reconstruct relative YM values with errors less than 10%. While the first phantom study showed that strain imaging led to better estimation of the inclusion's YM ratio, the difference is insignificant. The second phantom study demonstrated that the YM ratio accuracy is significantly higher than that of the strain imaging. Moreover, in both cases, qualitative assessment of the images indicates that the YM images are better representations of the known phantom geometries, including the tumor size and location. The comparable accuracy achieved by the proposed method compared to that of strain imaging in the phantom studies underestimates the improvement achieved by the proposed method considerably. This is due to the fact that with the phantom studies, the stress uniformity assumption is not as poor as it is in clinical cases. In fact, the significantly higher accuracy observed with the second phantom study can be well attributed to the fact that the second phantom has a more complex geometry which renders the stress uniformity assumption less valid compared to the first phantom. This was clearly observed in the clinical study where strain imaging in the second tumour region indicated YM ratio of 2.7 compared to 1.8 obtained from the proposed method. The latter is consistent with the YM ratio obtained for the first tumour region which showed YM ratio of 2.1. The small difference in the YM ratio obtained through the two different planes can be attributed to tumor inhomogeneity or systematic reconstruction errors. Overall, comparison of the reconstructed elasticity images with the clinical breast B-mode images indicate that the proposed method can detect cancerous regions reasonably accurately, with an extra benefit that it provides additional valuable information pertaining to the tumor relative stiffness which can serve as a quantitative biomarker for cancer diagnosis. Sources of YM reconstruction errors include errors in the estimated axial and lateral displacements used as boundary conditions. They also include stress calculation errors arising from idealizing the breasts 3D geometry into 2D geometry. While the phantom studies indicated that these errors are not of major magnitude, more advanced tissue motion tracking methods can be used to improve the accuracy of boundary conditions estimation. To further improve the stress calculation model, 3D automatic US breast imaging can be utilized [38], [39].

Among researchers working in the breast US elastography area, Goenezen et al. [40] applied a similar technique to distinguish fibroadenoma (solid benign lesions) from invasive ductal carcinomas (malignancies). For the boundary conditions of the tissue FOV, they applied measured axial displacements as prescribed boundary conditions. For lateral displacement boundary conditions, in contrast to our method which uses reasonably accurate lateral displacements measured using the RF data, they assumed that the tissue is free to move laterally along the four boundaries. As the authors stated, the latter free motion assumptions is inaccurate and can lead to artifacts in the constructed image. Based on their method nine out of ten studied tumors were correctly classified as either benign or malignant. In another breast elastography clinical study which included 939 breast masses,

Berg et al. [41] investigated the efficacy of elastography implemented in a prototypic US system equipped with shear-wave elastography (RUBI, prototype for Aixplorer, SuperSonic Imagine, France). Their aim was assessing the improvement of specificity of breast tumor detection with this system. Although quantitative, it was observed that the reproducibility of the method was low and the results were highly dependent to the operator. In our proposed system, we attempted to formulate the elasticity reconstruction problem based on reasonably solid physics as we considered both of the accurately measured axial and lateral displacements as boundary conditions. The results of the tissue mimicking phantom studies indicated that method is both accurate and reproducible. However, a larger clinical study including different lesion types is required to validate its efficacy in clinical setting. A potentially important application of the proposed breast elastography method is monitoring breast cancer degeneration in response to treatment [42]-[44]. Response to anti-cancer therapies including chemotherapy frequently alter biomechanical properties of tumor. Another interesting future study can be testing a hypothesis of having correlation between tumor stiffness and level of invasiveness.

Overall, the method proposed in this article involves a standard ultrasound imaging system with accessibility to its RF data. Unlike some other elastography systems, it does not involve extra hardware elements for mechanical stimulation or data acquisition. Moreover, the proposed elastography image reconstruction algorithm can be easily implemented, leading to a low cost system that can be potentially utilized as an effective clinical tool for breast cancer diagnosis or treatment response monitoring.

#### REFERENCES

- [1] Worldwide Breast Cancer. [www.worldwidebreastcancer.com](http://www.worldwidebreastcancer.com). Accessed January 25, 2017.
- [2] J. E. Joy, E. E. Penhoet, D. B. Petitti, "Saving Women's Lives: Strategies for Improving Breast Cancer Detection and Diagnosis," Institute of Medicine (US) and National Research Council (US) Committee on New Approaches to Early Detection and Diagnosis of Breast Cancer, Washington (DC), National Academies Press (US), 2005.
- [3] S. C. Rankin, "MRI of the breast," *Br. J. Radiol.*, vol. 73, no. 872, pp. 806-818, Aug. 2000.
- [4] Y. C. Fung, *Biomechanics: Mechanical Properties of Living Tissues*. 2<sup>nd</sup> ed., New York, NY, USA: Springer, 1981.
- [5] W. A. D. Anderson, *Pathology*. 5<sup>th</sup> ed., St. Louis, MO., USA: C. V. Mosby Co., 1953.
- [6] T. A. Krouskop, T. M. Wheeler, F. Kallel, B. S. Garra, and T. Hall, "Elastic Moduli of Breast and Prostate Tissues under Compression," *Ultrason. Imaging*, vol. 20, no. 4, pp. 260-274, Oct. 1998.
- [7] A. Samani and D. Plewes, "An inverse problem solution for measuring the elastic modulus of intact ex vivo breast tissue tumours," *Phys. Med. Biol.*, vol. 52, no. 5, pp. 1247-1260, Mar. 2007.
- [8] A. Samani and D. Plewes, "A method to measure the hyperelastic parameters of ex vivo breast tissue samples," *Phys. Med. Biol.*, vol. 49, no. 18, pp. 4395-405, Sep. 2004.
- [9] J. Ophir, "Elastography: A quantitative method for imaging the elasticity of biological tissues," *Ultrason. Imaging*, vol. 13, no. 2, pp. 111-134, Apr. 1991.
- [10] A. Evans, P. Whelehan, K. Thomson et al., "Quantitative shear wave ultrasound elastography: initial experience in solid breast masses," *Breast Cancer Res.*, vol. 12, no. 6, p. R104, Dec. 2010.
- [11] D. O. Cosgrove, W. A. Berg, C. J. Doré et al., "Shear wave elastography for breast masses is highly reproducible," *Eur. Radiol.*, vol. 22, no. 5, pp. 1023-1032, May 2012.

- [12] Z. L. Wang, J. L. Li, M. Li, Y. Huang, W. B. Wan, and J. Tang, "Study of quantitative elastography with supersonic shear imaging in the diagnosis of breast tumours," *Radiol. Med.*, vol. 118, no. 4, pp. 583–590, Jun. 2013.
- [13] S. H. Lee, J. M. Chang, W. H. Kim et al., "Differentiation of benign from malignant solid breast masses: comparison of two-dimensional and three-dimensional shear-wave elastography," *Eur. Radiol.*, vol. 23, no. 4, pp. 1015–1026, Apr. 2013.
- [14] E. B. Mendelson, J.-F. Chen, and P. Karstaedt, "Assessing tissue stiffness may boost breast imaging specificity," *Diagn. Imaging*, vol. 31, no. 12, pp. 15–17, 2009.
- [15] R. Sinkus, M. Tanter, T. Xydeas, S. Catheline, J. Bercoff, and M. Fink, "Viscoelastic shear properties of in vivo breast lesions measured by MR elastography," *Magn. Reson. Imaging*, vol. 23, no. 2, pp. 159–165, Feb. 2005.
- [16] R. Sinkus, J. Lorenzen, D. Schrader, M. Lorenzen, M. Dargatz, and D. Holz, "High-resolution tensor MR elastography for breast tumour detection," *Phys. Med. Biol.*, vol. 45, no. 6, pp. 1649–64, Jun. 2000.
- [17] E. E. W. Van Houten, M. M. Doyley, F. E. Kennedy, J. B. Weaver, and K. D. Paulsen, "Initial in vivo experience with steady-state subzone-based MR elastography of the human breast," *J. Magn. Reson. Imaging*, vol. 17, no. 1, pp. 72–85, Jan. 2003.
- [18] V. Egorov and A. P. Sarvazyan, "Mechanical Imaging of the Breast," *IEEE Trans. Med. Imaging*, vol. 27, no. 9, pp. 1275–1287, Sep. 2008.
- [19] B. S. Garra, E. I. Cespedes, J. Ophir et al., "Elastography of breast lesions: initial clinical results," *Radiology*, vol. 202, no. 1, pp. 79–86, Jan. 1997.
- [20] T. J. Hall, Y. Zhu, and C. S. Spalding, "In vivo real-time freehand palpation imaging," *Ultrasound Med. Biol.*, vol. 29, no. 3, pp. 427–35, Mar. 2003.
- [21] A. Thitaikumar, L. M. Mobbs, C. M. Kraemer-Chant, B. S. Garra, and J. Ophir, "Breast tumor classification using axial shear strain elastography: a feasibility study," *Phys. Med. Biol.*, vol. 53, no. 17, pp. 4809–4823, Sep. 2008.
- [22] M. Rao, S. Baker, A. M. Sommer, et al., "Shear strain elastography for breast mass differentiation," *7th International Conference on the Ultrasonic Measurement and Imaging of Tissue Elasticity*, Austin, TX, USA, 2008.
- [23] K. M. Hiltawsky, M. Krüger, C. Starke, L. Heuser, H. Ermert, and A. Jensen, "Freehand ultrasound elastography of breast lesions: clinical results," *Ultrasound Med. Biol.*, vol. 27, no. 11, pp. 1461–9, Nov. 2001.
- [24] E. S. Burnside, T. J. Hall, A. M. Sommer et al., "Differentiating Benign from Malignant Solid Breast Masses with US Strain Imaging," *Radiology*, vol. 245, no. 2, pp. 401–410, Nov. 2007.
- [25] D. M. Regner, G. K. Hesley, N. J. Hangiandreou et al., "Breast Lesions: Evaluation with US Strain Imaging—Clinical Experience of Multiple Observers," *Radiology*, vol. 238, no. 2, pp. 425–437, Feb. 2006.
- [26] M. M. Doyley, P. M. Meaney, and J. C. Bamber, "Evaluation of an iterative reconstruction method for quantitative elastography," *Phys. Med. Biol.*, vol. 45, no. 6, pp. 1521–1540, Jun. 2000.
- [27] A. A. Oberai, N. H. Gokhale, S. Goenezen, P. E. Barbone, T. J. Hall, A. M. Sommer, J. Jiang, "Linear and nonlinear elasticity imaging of soft tissue in vivo: demonstration of feasibility," *Phys. Med. Biol.*, vol. 54, no. 5, pp. 1191–1207, Mar. 2009.
- [28] A. Samani, J. Bishop, and D. B. Plewes, "A constrained modulus reconstruction technique for breast cancer assessment," *IEEE Trans. Med. Imaging*, vol. 20, no. 9, pp. 877–885, Sep. 2001.
- [29] H. Karimi, A. Fenster, and A. Samani, "A novel fast full inversion based breast ultrasound elastography technique," *Phys. Med. Biol.*, vol. 58, no. 7, pp. 2219–2233, Apr. 2013.
- [30] S. R. Mousavi, A. Sadeghi-Naini, G. J. Czarnota, and A. Samani, "Towards clinical prostate ultrasound elastography using full inversion approach," *Med. Phys.*, vol. 41, no. 3, p. 33501, Feb. 2014.
- [31] A. Samani, S. Shavakh, M. Amooshahi, S. R. Mousavi, "Breast linear and nonlinear real-time ultrasound elastography," *2nd International Conference on Computational & Mathematical Biomedical Engineering*, Washington DC, USA, 2011.
- [32] Y. Mei, S. Wang, X. Shen, S. Rabke, S. Goenezen, "Mechanics Based Tomography: A Preliminary Feasibility Study," *Sensors*, vol. 17, no. 5, May 2017.
- [33] A. A. Oberai, N. H. Gokhale, and G. R. Feij o, "Solution of inverse problems in elasticity imaging using the adjoint method," *Inverse Probl.*, vol. 19, no. 2, pp. 297–313, Apr. 2003.
- [34] H. Rivaz, E. M. Boctor, M. A. Choti, and G. D. Hager, "Real-Time Regularized Ultrasound Elastography," *IEEE Trans. Med. Imaging*, vol. 30, no. 4, pp. 928–945, Apr. 2011.
- [35] H. Rivaz, E. Boctor, P. Foroughi, R. Zellars, G. Fichtinger, and G. Hager, "Ultrasound Elastography: A Dynamic Programming Approach," *IEEE Trans. Med. Imaging*, vol. 27, no. 10, pp. 1373–1377, Oct. 2008.
- [36] E. L. Madsen, M. A. Hobson, H. Shi, T. Varghese, and G. R. Frank, "Tissue-mimicking agar/gelatin materials for use in heterogeneous elastography phantoms," *Phys. Med. Biol.*, vol. 50, no. 23, pp. 5597–5618, Dec. 2005.
- [37] G. R. Joldes, A. Wittek, and K. Miller, "Real-time nonlinear finite element computations on GPU – Application to neurosurgical simulation," *Comput. Methods Appl. Mech. Eng.*, vol. 199, no. 49, pp. 3305–3314, 2010.
- [38] D. Kotsianos-Hermle, S. Wirth, T. Fischer, K. M. Hiltawsky, and M. Reiser, "First clinical use of a standardized three-dimensional ultrasound for breast imaging," *Eur. J. Radiol.*, vol. 71, no. 1, pp. 102–108, Jul. 2009.
- [39] A. Fenster, G. Parraga, and J. Bax, "Three-dimensional ultrasound scanning," *Interface Focus*, vol. 1, no. 4, 2011.
- [40] S. Goenezen, J. F. Dord, Z. Sink et al., "Linear and Nonlinear Elastic Modulus Imaging: An Application to Breast Cancer Diagnosis," *IEEE Trans. Med. Imaging*, vol. 31, no. 8, pp. 1628–1637, Aug. 2012.
- [41] W. A. Berg, D. O. Cosgrove, C. J. Doré et al., "Shear-wave Elastography Improves the Specificity of Breast US: The BE1 Multinational Study of 939 Masses," *Radiology*, vol. 262, no. 2, pp. 435–449, Feb. 2012.
- [42] O. Falou O, A. Sadeghi-Naini, S. Prematilake et al., "Evaluation of neoadjuvant chemotherapy response in women with locally advanced breast cancer using ultrasound elastography," *Transl. Oncol.*, vol. 6, no. 1, pp. 17–24, Feb. 2013.
- [43] A. Sadeghi-Naini, N. Papanicolau, O. Falou et al., "Quantitative Ultrasound Evaluation of Tumor Cell Death Response in Locally Advanced Breast Cancer Patients Receiving Chemotherapy," *Clin. Cancer Res.*, vol. 19, no. 8, pp. 2163–2174, Apr. 2013.
- [44] L. Sannachi, H. Tadayyon, A. Sadeghi-Naini et al., "Non-invasive evaluation of breast cancer response to chemotherapy using quantitative ultrasonic backscatter parameters," *Med. Image Anal.*, vol. 20, no. 1, pp. 224–236, Feb. 2015.